HHS Public Access

Author manuscript

Cytometry A. Author manuscript; available in PMC 2021 October 01.

Published in final edited form as:

Cytometry A. 2020 October ; 97(10): 1081–1089. doi:10.1002/cyto.a.24037.

Imaging Flow Cytometry Analysis of CEACAM Binding to Opa-Expressing *Neisseria gonorrhoeae*

Lacie M. Werner[#1], **Allison Palmer**[#1], **Asya Smirnov**[1], **Meagan Belcher Dufrisne**[2], **Linda Columbus**[2], **Alison K. Criss**[1,*]

[1]Department of Microbiology, Immunology, and Cancer Biology, University of Virginia, Charlottesville, Virginia, 22903

[2]Department of Chemistry, University of Virginia, Charlottesville, Virginia, 22903

[#] These authors contributed equally to this work.

Abstract

Human carcinoembryonic antigen-related cell adhesion molecules (CEACAMs) are a family of receptors that mediate intercellular interactions. Pathogenic bacteria have ligands that bind CEACAMs on human cells. *Neisseria gonorrhoeae* (Gc) encodes numerous unique outer membrane opacity-associated (Opa) proteins that are ligands for one or more CEACAMs. CEACAMs that are expressed on epithelial cells facilitate Gc colonization, while those expressed on neutrophils affect phagocytosis and consequent intracellular survival of Gc. Since Opa protein expression is phase-variable, variations in receptor tropism affect how individual bacteria within a population interact with host cells. Here we report the development of a rapid, quantitative method for collecting and analyzing fluorescence intensity data from thousands of cells in a population using imaging flow cytometry to detect N-CEACAM bound to the surface of Opa-expressing Gc. We use this method to confirm previous findings regarding Opa-CEACAM interactions and to examine the receptor—ligand interactions of Gc expressing other Opa proteins, as well as for other N-CEACAM proteins.

Keywords

imaging flow cytometry; carcinoembryonic antigen-related cell adhesion molecule (CEACAM); Neisseria gonorrhoeae; Opa protein; receptor-ligand binding

Human carcinoembryonic antigen-related cell adhesion molecules (CEACAMs) are a family of 12 receptors with distinct expression patterns on different cell types. Each CEACAM has unique ligand binding capacities, and some CEACAMs have activating or inhibitory cytosolic signaling motifs, while others have no cytosolic tail and contain glycosylphosphatidylinositol (GPI) anchors in the membrane. Thus, the consequence of an

[*]Correspondence to: Alison K. Criss, Department of Microbiology, Immunology, and Cancer Biology, University of Virginia School of Medicine, Charlottesville, VA 22908-0734, akc2r@virginia.edu.

Additional Supporting Information may be found in the online version of this article.

Conflict of Interest

The authors have no conflict of interest.

interaction between a CEACAM and a potential ligand is dependent on which CEACAM is engaged (1).

CEACAMs are exploited by pathogenic bacteria during infection (2). Examples of pathogens with ligands that bind CEACAMs are *Moraxella catarrhalis* (UspA protein), *Haemophilus influenzae* (OmpP1 protein), *Escherichia coli* (Dr adhesins), and *Neisseria gonorrhoeae* (Opa proteins) (3–5). *N. gonorrhoeae* (Gc) is an obligate human pathogen that causes the sexually transmitted infection gonorrhea. Gc interacts with CEACAMs via outer membrane opacity-associated (Opa) proteins. Each strain of Gc encodes 10 or more *opa* genes, which undergo recombination and mutation to diversify within and among strains (6). Each Opa is phase-variable, such that a single strain can express anywhere from zero to multiple Opa proteins. Gc recovered from infected individuals is predominantly Opa expressors (7). Most Opa proteins in a strain are ligands for one or more human CEACAMs. Receptor binding cannot be predicted from the Opa primary sequence and is instead dictated by structural characteristics of Opa extracellular loops (8).

CEACAM engages Opa proteins through an extracellular N-terminal immunoglobulin fold (9–11). CEACAM-Opa binding allows Gc to engage both epithelial cells and neutrophils during infection of the host (9). Characterizing the CEACAM binding profiles of diverse Opa proteins from different strains contributes to our understanding of how Gc interacts with CEACAM-bearing cells to cause productive infection.

Various methods have been used to determine the specificity and selectivity of Opa-CEACAM interactions. Opa binding to CEACAMs that are expressed on the membrane of HeLa cells and CHO cells has been assessed by Western blot, fluorescence microscopy, immunoelectron microscopy, and microtiter plate-based fluorescent detection of bound bacteria (12–17). While mammalian cell lines are a relevant model for host-Gc interactions, the potential for interference by other receptors on the cell surface can confound conclusions about the CEACAM binding capacity of Opa proteins. An alternative approach is to use cell-free purified CEACAMs expressed as fusions to GFP (18–21) or Fc tag (22) that are incubated with Gc and other bacteria expressing Opa proteins, with CEACAM binding assessed by flow cytometry. Previously, our group evaluated Opa-CEACAM interactions by the ability of Gc to bind recombinantly expressed N-terminus of CEACAM (N-CEACAM). In that assay, the bacteria were incubated with various N-CEACAMs, the supernatant and bacterial pellet were collected and separated by SDS-PAGE, and the N-CEACAM partitioning to the pellet was analyzed by immunoblotting with pan-CEACAM antibody (23). However, this method was subject to variation due to gel loading, blot transfer, and background bands due to nonspecific antibody binding, was time-consuming, and reported results for the whole Gc population rather than on a single-bacterium basis.

Here we report an approach to define Opa-mediated interactions with recombinant N-CEACAM by using imaging flow cytometry, which offers advantages over conventional flow cytometry. The primary advantage is that given the small size of Gc (0.5 μm diameter as a monococcus and 1 μm as a diplococcus), conventional flow cytometry requires customization and/or extensive calibration and standardization to avoid inaccurate measurements of submicron particles (24–27). In contrast to conventional flow cytometry

where single particles are detected bases on a signal threshold, imaging flow cytometry instead identifies objects based on pixel intensities of the particle images that are above background intensity, allowing for accurate detection of bacteria this size. Furthermore, imaging flow cytometry, but not conventional flow cytometry, makes it more straightforward to exclude bacterial aggregates that could skew the MFI of the whole bacterial population that is analyzed. Theoretically, this approach can be extended to other CEACAM-binding bacteria, and more generally to any ligand—receptor interaction where one of the interacting partners can be made into a soluble fragment.

Materials and Methods

Creation of Recombinant N-CEACAMs 4, 5, 6, and 8

Coding sequences for the recombinant expression of N-CEACAM were synthesized and subcloned into the pGEX-2T vector (containing a glutathione S-transferase (GST)-tag) by GenScript. The constructs were designed so that the N-terminal GST tag is separated from the CEACAM domain by a TEV cleavage site as and a short linker (of the amino acid sequence GGA) as previously reported (23). Plasmids from GenScript were confirmed by Sanger sequencing with forward and reverse primers.

Site Directed Mutagenesis for the Creation of CEACAM1-I87A/Q89A/I91A

Three rounds of PIPE site directed mutagenesis were performed in sequence for the three different mutations introduced. For each round, PIPE-PCR was performed as previously described (28). *E. coli* Top 10 cells were transformed with the resulting amplicon. DNA was purified using the QiaPrep Spin Miniprep Kit (Qiagen) and mutations were confirmed by Sanger sequencing (Genewiz). The primers for mutagenesis are as follows:

CEACAM1-T87A-F:

TTCTACGCACTACAAGTCATAAAGTCAGATCTTGTG

CEACAM1-T87A-R:

TTGTAGTGCGTAGAATCCTGTGTCATTCTGGGTGAC

CEACAM1-_89A-F:

GCACTAGCAGTCATAAAGTCAGATCTTGTGAATGAA

CEACAM1-_89A-R:

TATGACTGCTAGTGCGTAGAATCCTGTGTCATTCTG

CEACAM1-_91A-F:

GCAGTCGCAAAGTCAGATCTTGTGAATGAAGAAGCA

CEACAM1-_91A-R:

TGACTTTGCGACTGCTAGTGCGTAGAATCCTGTGTC

GST-CEACAM Protein Purification

Recombinant protein was expressed and purified as previously described for the N-terminal domains of CEACAM 1 and 3 (23) using the pGEX-2T vector containing GST-tagged N-terminal domains of CEACAM1, 3, 4, 5, 6, and 8. All proteins were prepared in a final buffer of 20 mM Tris, pH 8.0, 500 mM sodium chloride and 10% glycerol and brought to a final concentration between 4 and 6 mg/ml using an Amicon Ultra Centrifugal Filter Unit with a 10,000 MWCO (Millipore). Purified GST-CEACAM proteins were stored for at −80°C. GST-CEACAM protein yields ranged between 0.5 and 12 mg protein per liter of *E. coli* culture.

Gc Isolates and Growth Conditions

All Gc isolates are in an FA1090 strain background. Opaless Gc in which all native *opa* genes were deleted was previously described (29). OpaD+ Gc, Opa50+ Gc, and Opa60+ Gc contain non-phase-variable, constitutively expressed versions of each *opa* gene, cloned into the native *opaD* locus of Opaless Gc (23). An FA1090 Gc strain with a non-phase-variable, IPTG-inducible expressed *opa54* gene was created. *opa54* was amplified out of strain N2027 (strain kindly provided by Scott Gray-Owen, University of Toronto). The *opa54* gene already contained a non-phase-variable signal sequence. Restriction enzyme sites (XbaI and SacI) were added to the *opa54* amplicon for ligation into the Gc complementation plasmid pKH35 (30) using forward primer AAATTCTAGATCCAAGGAGCCGAA and reverse primer AAAACTCGAGTCAGAAGCGGTAGCG. Both the PCR product and plasmid were digested with XbaI and SacI, ligated together, and transformed into TOP 10 *E. coli*. Proper insertion of *opa54* into pKH35 was confirmed by restriction digest and DNA sequencing using the primers above (Genewiz). pKH35 with *opa54* was transformed into Opaless Gc and selected for by chloramphenicol resistance at 0.5 μg/ml. Opa54 expression was confirmed by Western blot using the 4B12 anti-Opa antibody after growth of Opa54+ Gc on GCB plates containing 1 mM IPTG. All Gc were grown overnight on GCB plates containing Kellogg's supplements I and II at 37°C and 5% CO_2, except Opa54+ Gc, where plates additionally contained 1 mM IPTG to induce Opa54 expression.

Opa-CEACAM Pulldown

Protein concentration of N-CEACAMs were measured by absorbance at 280 nm. On the day of the assay, N-CEACAMs were diluted in 500 μl to the indicated final concentration per sample in RPMI with 10% FBS (RPMI-10). Gc were collected from GCB plates, normalized to a concentration of 1×10^8 CFU/ml, washed once in 1x PBS containing 5 mM $MgSO_4$, and resuspended in the N-CEACAM-RPMI-10 solution. Gc and the CEACAM solution were incubated with end over end rotation for 30 min at 37°C with 5% CO_2. After incubation, bacteria were pelleted at 10,000g and washed twice in 1× PBS with 5 mM $MgSO_4$.

Bacterial Staining

Gc were resuspended in 75 μl 0.5 μg/ml mouse anti-GST monoclonal antibody clone p1A12 (Biolegend, San Diego, CA) in RPMI-10 and incubated at 37°C for 30 min. Bacteria were pelleted at 10,000*g* for 3 min at room temperature, and the supernatant was discarded. The bacterial pellet was resuspended in 75 μl of 5 μg/ml goat anti-mouse AF488 (Invitrogen, Carlsbad, CA) in RPMI with 10% FBS and incubated for 30 min at 37°C. Bacteria were pelleted at 10,000*g* for 3 min at room temperature, and the supernatant was discarded. Gc were then resuspended in 2% paraformaldehyde (PFA) containing 5 μg/ml 4′,6-diamidino-2-phenylindole (DAPI) DNA stain.

Data Acquisition

Samples were analyzed by imaging flow cytometry using Imagestream^X Mk II with INSPIRE® software (Luminex Corporation). Alexa Fluor®488 fluorescence was detected with excitation at 488 nm and emission collected with a 480–560 nm filter. DAPI fluorescence was detected with excitation at 405 nm and emission collected with a 420–505 nm filter. For each sample, a laser LED intensity of 40.59 mW was used for brightfield 1 and the emission was collected with a 420–480 nm filter; a laser LED intensity 55.00 mW was used for brightfield 2 and the emission collected with a 570–595 nm filter. Compensation matrices to remove spectral overlap were calculated for each experiment using DAPI+ bacteria without addition of αGST/αMsAF488, and non-DAPI-labeled OpaD+ Gc bound to N-CEACAM1 with αGST/αMsAF488 (see Supporting information Data S1).

Data Analysis

Data analysis was performed using IDEAS® v6.2 software (Luminex Corporation). The gating strategy for data analysis using this software is outlined in Figure 1. A compensation matrix was created from the single-color controls: bacteria singly positive for AF488 or DAPI. This compensation matrix was applied to all files from the experiment. From the DAPI intensity histogram, DAPI+ bacteria were identified (Fig. 1A). A scatter plot with area on the *x*-axis and aspect ratio on *y*-axis was generated, and single particles (“singlets”) were identified by gating on the cell population with high aspect ratio (>0.2) and low area (<20) (Fig. 1B,C). A histogram of brightfield gradient root mean square (RMS) was generated for single DAPI+ bacteria and focused bacteria were identified as a cell population with high (≥52) gradient RMS (Fig. 1D–F). Within the gate, the population with RMS < 65 was not different in MFI for AF488 than the population RMS > 65 (4,718.38 vs. 4,506.08, respectively). A histogram of AF488 intensity for the population of single DAPI+ focused bacteria was created (Fig. 1G–I). A gate was created in this histogram to identify the CEACAM+ Gc population. The gating strategy needs to be experimentally determined by each user, by setting the positive gate above the intensity of the cell population in the negative control.

Statistics

Comparisons between single Gc isolates for a given CEACAM were performed using one-way ANOVA with post hoc multiple comparisons. Comparisons between fluorescence on OpaD+ Gc after incubation with N-CEACAM1 compared to the addition of no CEACAM or

a triple mutant N-CEACAM1 were performed using a Student's unpaired *t* test. Comparisons between N-CEACAM1 binding to OpaD+ Gc and Opaless Gc were performed using a Student's unpaired *t* test.

Results

Confirmation of a Specific Interaction between Opa and CEACAM by Imaging Flow Cytometry

We developed an imaging flow cytometry-based method to analyze the CEACAM-binding profiles of Gc expressing an Opa protein of interest. In this assay, Gc is incubated with N-CEACAM. A protocol for protein expression and purification of recombinant GST-tagged N-CEACAMs was previously optimized (23). N-CEACAM was recombinantly expressed as a GST-fusion because we previously found the GST moiety prevented N-CEACAM aggregation. The N-CEACAM remaining bound to Gc after washing is detected with an anti-GST antibody, followed by AlexaFluor 488 (AF488)-labeled anti-mouse IgG. Gc was detected with DAPI. The Gc suspension is examined by imaging flow cytometry by gating on DAPI+, focused particles and quantifying AF488 fluorescence in this gate (Fig. 1). Data are expressed as percent of bacteria that are AF488 positive (Fig. 2a) and as MFI of AF488 fluorescence (Fig. 2b) for all particles.

The imaging flow cytometry method was first developed using OpaD+ Gc and N-CEACAM1; we previously reported that OpaD binds to CEACAM1 (23) (Fig. 2). Binding of N-CEACAM-1 by OpaD+ Gc was significantly higher by percentage and MFI than binding to Opaless due to the specific interaction of the OpaD protein on Gc and recombinant N-CEACAM1. Several technical and biological controls were employed to validate the specificity of the Opa-CEACAM interaction. (1) In the absence of N-CEACAM1, OpaD+ Gc had minimal AF488+ Gc, i.e. fluorescence from nonspecific binding of α-GST and α-MsAF488 to OpaD+ Gc, showing that fluorescence only occurs when CEACAM is present on the measured bacteria. (2) To determine the necessity for Opa expression on Gc to allow CEACAM binding, we showed that for Opaless Gc, percentage AF488+ and fluorescence were not significantly different from the no-CEACAM negative control. (3) The percentage AF488+ and MFI of OpaD+ Gc incubated with recombinant GST was not significantly different from the no-CEACAM negative control, further confirming that the interaction being measured is CEACAM-Opa, not GST-Opa. (4) N-CEACAM1 with three point mutations in the Opa binding interface (CEACAM1-I87A/Q89A/I91A (31)) was no different in interaction with OpaD+ Gc than the non-CEACAM negative control in percentage AF488+ Gc or MFI. Together, these results demonstrate that Gc specifically binds to CEACAM using Opa as a ligand, and support the use of imaging flow cytometry to examine this interaction.

Titration of N-CEACAMs Using OpaD+ Gc

We used the imaging flow cytometry assay to titrate each of several GST-tagged human N-CEACAMs for OpaD+ Gc. The percentage of AF488+ Gc was determined at varying concentrations of each N-CEACAM (Fig. 3). Based on our previous report (23), we predicted OpaD+ Gc would bind to CEACAM1 and 3, and anticipated binding to additional

CEACAMs. Opaless Gc was used as a control for nonspecific binding at the highest concentration of each N-CEACAM (Fig. 4). Binding was evaluated as percent of bacteria that were AF488+.

N-CEACAMs 1 and 5 bound to OpaD+ Gc at low μM concentrations (0.4 and 0.2 μM, respectively). In comparison, maximal N-CEACAM3 binding was achieved at 12 μM. CEACAMs 4, 6, and 8 bound poorly to OpaD+ Gc (less than 25%, 10%, and 15% AF488+ Gc, respectively). At these concentrations, no specific binding to Opaless Gc was measured. While these titrations were reproducible for the N-CEACAM preparations used here, each preparation must be optimized for Opa-CEACAM binding based on a similar concentration titration.

CEACAM Binding by Each of Four Opa Proteins

To characterize the CEACAM binding of other Opas, we selected a concentration at which a CEACAM bound to OpaD. If there was no appreciable binding of OpaD to the N-CEACAM, we selected the highest concentration tested (Fig. 3). Using these concentrations, the CEACAM binding profiles for Gc expressing OpaD from strain FA1090 or Opa50, Opa54, or Opa60 from strain MS11 were determined by imaging flow cytometry. Opaless Gc incubated with the indicated CEACAM served as a negative control for background AF488+ fluorescence on bacteria, as we have previously shown Opaless Gc does not bind CEACAMs (Fig. 2) (23). Multiple previous reports have shown that OpaD+ (23), Opa54+ (32), and Opa60+ Gc (10, 17, 23) can bind to CEACAM1, and in agreement, we saw significant binding of CEACAM1 to OpaD+, Opa54+, and Opa60+ Gc (Fig. 4a). Similarly, OpaD+ (23) and Opa60+ Gc (10, 17, 23) were reported to bind to CEACAM3, and in agreement, we saw significant binding of CEACAM 3 to OpaD+ and Opa60+ Gc (Fig. 4b). Previous literature has indicated that no Opas bind to CEACAM4 (33, 34). Using our assay, only Opa50+ Gc bound at significant, albeit low, levels to CEACAM4 (Fig. 4c). Most CEACAM-binding Opas have been reported to bind CEACAM5 (32), and in agreement, we found that OpaD+ and Opa60+ Gc both bound to CEACAM5 (Fig. 4d). Additionally, Opa60+ Gc bound significantly to CEACAM6, as previously reported (13) (Fig. 4e). Finally, no Opas have been reported to bind CEACAM8 (12, 13, 15). Here, only Opa50+ Gc bound CEACAM8 at low levels that were significantly above Opaless background (Fig. 4f).

The overall consensus between the imaging flow cytometry results and previous publications using other methods supports the use of this assay to rapidly and quantitatively measure the CEACAM binding profile of multiple Opa proteins.

Discussion

The goal of this project was to create and optimize a straightforward, rapid, specific method for determining bacterial ligand—host receptor interactions by imaging flow cytometry, using Gc Opa proteins and human CEACAMs. Compared with our previous immunoblot-based method (23), imaging flow cytometry allows gating on single, intact bacteria, such that differences within a population can be evaluated and complications with SDS-PAGE and transfer are avoided. Further, the use of recombinant N-CEACAM in the current approach avoids the complications faced by CEACAM expression in mammalian cell lines,

such as efficiency of CEACAM expression, expression of multiple splice variants, and confounding results due to expression of endogenous CEACAM(s). Furthermore, compared to conventional flow cytometry methods, imaging flow cytometry allows single submicron size bacteria to be reliably identified, without customizing and calibrating a conventional flow cytometer, which may not be feasible in a multiuser core facility (24, 35).

We used this approach to measure specific and selective interactions between four different Opa proteins and the N-terminal domains of six different CEACAMs. Gating on single, DAPI+ bacteria ensured that all positive signal detected is from CEACAM bound to intact bacteria, and not from a dimerized protein or protein aggregates that nonspecifically pellet along with the bacteria. When selecting for in focus bacteria, we noted two populations in the gate that have $52 < RMS < 65$ and $66 < RMS < 78$, but since they have the same MFI for AF488 (see Materials and Methods), they do not affect interpretation of results regarding ability of Opa + bacteria to bind GST-N-CEACAM. At this time, we do not know what is responsible for the difference in RMS, but could be due to stage of bacterial growth and/or monococcal vs. diplococcal form. Importantly, CEACAMs do not bind bacteria that do not express Opa proteins, neither the GST antibody or GST alone bind Opa + Gc, and mutation of key residues in the CEACAM1-Opa binding interface prevents Opa-Gc interaction (Fig. 2). Our results generally correspond to the selectivity of CEACAM-dependent binding of these particular Opa + Gc reported by us (23) and others (10, 14, 17, 21, 23, 32, 33, 36, 37). Moreover, we found that OpaD+ Gc interacts with CEACAM5, an epithelial CEACAM, which agrees with our observation that OpaD+ Gc binds avidly to epithelial cells (38). Thus, the imaging flow cytometry approach confirms known Opa-CEACAM interactions.

Understanding the selectivity of CEACAM binding to Opa allows us to infer which signaling pathways may be active in the context of host—pathogen interactions. For example, the cytoplasmic tail of CEACAM1 contains an immunoreceptor tyrosine based inhibitory motif (ITIM). ITIM signaling in most cell types relies on activation of SHP-1 and SHP-2 to inhibit cellular activity (39). In neutrophils, this could mean that antimicrobial activity is inhibited by ligand binding to CEACAM1. CEACAM3 is expressed solely on granulocytes like neutrophils. It is thought to be a decoy receptor that pathogenic bacteria bind with the same ligands they use to bind CEACAMs that promote infection (40). Polymorphisms in the CEACAM3 amino acid sequence allow for recognition of a spectrum of bacterial pathogens among human subpopulations (41). CEACAM3 has an ITAM domain in its C-terminus, and this is thought to cause the activation of neutrophils and bacterial killing. Knowing which ligands are able to bind to this specific CEACAM could be important in understanding why some pathogens are killed by granulocytes and others are not.

Previous reports have shown that neither CEACAM4 or CEACAM8 bind to any Opa proteins (33, 34). In this study, low yet statistically significant percentages of Opa50+ Gc were positive for CEACAM4 and for CEACAM8. CEACAM4 is hypothesized to be an “orphan” granulocyte receptor that does not interact with bacterial ligands, although the C-terminal ITAM retains the ability to drive bacterial internalization (34). It is important to note that our system is using nonglycosylated N-CEACAM, which could explain the

discrepancy of our results with previous literature. Future studies looking at glycosylated CEACAM4 and CEACAM8 could describe if and how this interaction occurs biologically.

While this method was developed to investigate the binding and selectivity between Opa proteins and CEACAMs, it can be extended to other systems and can be modified for other applications and labeling approaches. Technical variations of this assay could include the use of a fluorophore conjugated to the primary antibody against the recombinant protein of interest or a tagged protein. Further, since we were able to titrate the CEACAM fluorescence based on concentration of N-CEACAM protein, this assay could be performed as a competition assay where the presence of a competitor will affect the binding of the primary protein of interest, resulting in a loss of signal. Competition assays would help elucidate physiologically relevant questions, such as the affinity of one ligand over another. In this study, we used Opa proteins as the ligand of CEACAM, but there are other types of interactions for which this assay can be used, including other pathogens that are CEACAM-dependent like *M. catarrhalis* (UspA) and *H. influenzae* (OmpP1) (3, 4). More broadly, this system can be adapted to any receptor-ligand pair where one component is presented in its native conformation on the surface of a particle that is of the appropriate size and fluorescence for imaging flow cytometry, and its partner is soluble, in a functional conformation for binding, and can be followed with a fluorescent label. The speed, sensitivity, and throughput of imaging flow cytometry make this an effective approach for analysis of binding to small particles like bacteria.

Supplementary Material

Refer to Web version on PubMed Central for supplementary material.

Acknowledgments

We thank the UVA Flow Cytometry Core Facility, particularly Director Michael Solga and former Director Joanne Lannigan, for their assistance with imaging flow cytometry and critical review of the gating strategy. Raw imaging flow cytometry data are deposited in the FlowRepository:

RvFrpHL88bgf8ynmgzAK5H9LvUhizOVdqDkOX7a0QsUbxSZqtL4vy6qnhC9xEZ7S

RvFrBMnG7UmO3UzOB1Z1xhISRJK61rpjLEcKOIXNCidLiIM1Vxu24pOF7kPZsV8K

Grant sponsor: National Institute of Allergy and Infectious Diseases, Grant numberR01 AI097312, Grant numberT32 AI007046; Grant sponsor: National Institute of General Medical Sciences, Grant numberR35 GM131829

LITERATURE CITED

1. Tchoupa AK, Schuhmacher T, Hauck CR. Signaling by epithelial members of the CEACAM family — Mucosal docking sites for pathogenic bacteria. Cell Commun Signal 2014;12:27. [PubMed: 24735478]
2. Muenzner P, Rohde M, Kneitz S, Hauck CR. CEACAM engagement by human pathogens enhances cell adhesion and counteracts bacteria-induced detachment of epithelial cells. J Cell Biol 2005;170(5):825–836. [PubMed: 16115956]
3. Conners R, Hill DJ, Borodina E, Agnew C, Daniell SJ, Burton NM, Sessions RB, Clarke AR, Catto LE, Lammie D, et al. The Moraxella adhesin UspA1 binds to its human CEACAM1 receptor by a deformable trimeric coiled-coil. EMBO J 2008;27(12):1779–1789. [PubMed: 18497748]

4. Tchoupa AK, Lichtenegger S, Reidl J, Hauck CR. Outer membrane protein P1 is the CEACAM-binding adhesin of *Haemophilus influenzae*. Mol Microbiol 2015;98(3): 440–455. [PubMed: 26179342]
5. Korotkova N, Yang Y, le Trong I, Cota E, Demeler B, Marchant J, Thomas WE, Stenkamp RE, Moseley SL, Matthews S. Binding of Dr adhesins of *Escherichia coli* to carcinoembryonic antigen triggers receptor dissociation. Mol Microbiol 2008;67(2):420–434. [PubMed: 18086185]
6. Murphy GL, Connell TD, Barritt DS, Koomey M, Cannon JG. Phase variation of gonococcal protein II: Regulation of gene expression by slipped-strand mispairing of a repetitive DNA sequence. Cell 1989;56(4):539–547. [PubMed: 2492905]
7. Jerse AE, Cohen MS, Drown PM, Whicker LG, Isbey SF, Seifert HS, Cannon JG. Multiple gonococcal opacity proteins are expressed during experimental urethral infection in the male. J Exp Med 1994;179(3):911–920. [PubMed: 8113683]
8. de Jonge MI, Hamstra HJ, van Alphen L, Dankert J, van der Ley P. Mapping the binding domains on meningococcal Opa proteins for CEACAM1 and CEA receptors. Mol Microbiol 2003;50(3):1005–1015. [PubMed: 14617157]
9. Sadarangani M, Pollard AJ, Gray-Owen SD. Opa proteins and CEACAMs: Pathways of immune engagement for pathogenic *Neisseria*. FEMS Microbiol Rev 2011;35(3):498–514. [PubMed: 21204865]
10. Bos MP, Kao D, Hogan DM, Grant CCR, Belland RJ. Carcinoembryonic antigen family receptor recognition by gonococcal Opa proteins requires distinct combinations of hypervariable Opa protein domains. Infect Immun 2002;70(4):1715–1723. [PubMed: 11895933]
11. Fedarovich A, Tomberg J, Nicholas RA, Davies C. Structure of the N-terminal domain of human CEACAM1: Binding target of the opacity proteins during invasion of *Neisseria meningitidis* and *N. gonorrhoeae*. Acta Crystallogr D Biol Crystallogr 2006;62(Pt 9):971–979. [PubMed: 16929097]
12. Bos MP, Grunert F, Belland RJ. Differential recognition of members of the carcinoembryonic antigen family by Opa variants of *Neisseria gonorrhoeae*. Infect Immun 1997;65(6):2353–2361. [PubMed: 9169774]
13. Gray-Owen SD, Lorenzen DR, Haude A, Meyer TF, Dehio C. Differential Opa specificities for CD66 receptors influence tissue interactions and cellular response to *Neisseria gonorrhoeae*. Mol Microbiol 1997;26(5):971–980. [PubMed: 9426134]
14. Gray-Owen SD, Dehio C, Haude A, Grunert F, Meyer TF. CD66 carcinoembryonic antigens mediate interactions between Opa-expressing *Neisseria gonorrhoeae* and human polymorphonuclear phagocytes. EMBO J 1997;16(12):3435–3445. [PubMed: 9218786]
15. Chen T, Grunert F, Medina-Marino A, Gotschlich EC. Several carcinoembryonic antigens (CD66) serve as receptors for gonococcal opacity proteins. J Exp Med 1997;185(9):1557–1564. [PubMed: 9151893]
16. Bos MP, Hogan D, Belland RJ. Homologue scanning mutagenesis reveals CD66 receptor residues required for neisserial Opa protein binding. J Exp Med 1999;190(3):331–340. [PubMed: 10430622]
17. Bos MP, Kuroki M, Krop-Watorek A, Hogan D, Belland RJ. CD66 receptor specificity exhibited by neisserial Opa variants is controlled by protein determinants in CD66 N-domains. Proc Natl Acad Sci U S A 1998;95(16):9584–9589. [PubMed: 9689124]
18. Kuespert K, Weibel S, Hauck CR. Profiling of bacterial adhesin—host receptor recognition by soluble immunoglobulin superfamily domains. J Microbiol Methods 2007; 68(3):478–485. [PubMed: 17126432]
19. Kuespert K, Hauck CR. Characterizing host receptor recognition by individual bacterial pathogens. Methods Mol Biol 2009;470:57–65. [PubMed: 19089375]
20. Koniger V, Holsten L, Harrison U, Busch B, Loell E, Zhao Q, Bosnor DA, Roth A, Kengmo-Tchopa A, Smith SI, et al. *Helicobacter pylori* exploits human CEACAMs via HopQ for adherence and translocation of CagA. Nat Microbiol 2016;2:16188. [PubMed: 27748756]
21. Roth A, Mattheis C, Muenzner P, Unemo M, Hauck CR. Innate recognition by neutrophil granulocytes differs between *Neisseria gonorrhoeae* strains causing local or disseminating infections. Infect Immun 2013;81(7):2358–2370. [PubMed: 23630956]

22. Javaheri A, Kruse T, Moonens K, Mejias-Luque R, Debraekeleer A, Asche CI, Tegtmeyer N, Kalali B, Bach NC, Sieber SA, et al. *Helicobacter pylori* adhesin HopQ engages in a virulence-enhancing interaction with human CEACAMs. Nat Microbiol 2016;2:16189. [PubMed: 27748768]
23. Martin JN, Ball LM, Solomon TL, Dewald AH, Criss AK, Columbus L. Neisserial Opa protein-CEACAM interactions: Competition for receptors as a means of bacterial invasion and pathogenesis. Biochemistry 2016;55(31):4286–4294. [PubMed: 27442026]
24. Erdbrügger U, Rudy CK, Etter EM, Dryden KA, Yeager M, Klibanov AL, Lannigan J. Imaging flow cytometry elucidates limitations of microparticle analysis by conventional flow cytometry. Cytometry Part A 2014;85A(9):756–770.
25. Konokhova AI, Chernova DN, Moskalensky AE, Strokotov DI, Yurkin MA, Chernyshev AV, Maltsev VP. Super-resolved calibration-free flow cytometric characterization of platelets and cell-derived microparticles in platelet-rich plasma. Cytometry Part A 2016;89A(2):159–168.
26. Stoner SA, Duggan E, Condello D, Guerrero A, Turk JR, Narayanan PK, Nolan JP. High sensitivity flow cytometry of membrane vesicles. Cytometry Part A 2016;89A (2):196–206.
27. Groot Kormelink T, Arkesteijn GJA, Nauwelaers FA, van den Engh G, Nolte-'t Hoen ENM, Wauben MHM. Prerequisites for the analysis and sorting of extracellular vesicle subpopulations by high-resolution flow cytometry. Cytometry Part A 2016;89A(2):135–147.
28. Klock HE, Lesley SA. The polymerase incomplete primer extension (PIPE) method applied to high-throughput cloning and site-directed mutagenesis. Methods Mol Biol 2009;498:91–103. [PubMed: 18988020]
29. Ball LM, Criss AK. Constitutively Opa-expressing and Opa-deficient *Neisseria gonorrhoeae* strains differentially stimulate and survive exposure to human neutrophils. J Bacteriol 2013;195(13):2982–2990. [PubMed: 23625842]
30. Dillard JP. Genetic manipulation of *Neisseria gonorrhoeae*. Curr Protoc Microbiol 2011;Chapter 4:Unit4A 2.
31. Virji M, Evans D, Hadfield A, Grunert F, Teixeira AM, Watt SM. Critical determinants of host receptor targeting by *Neisseria meningitidis* and *Neisseria gonorrhoeae*: Identification of Opa adhesiotopes on the N-domain of CD66 molecules. Mol Microbiol 1999;34(3):538–551. [PubMed: 10564495]
32. Sintsova A, Wong H, MacDonald KS, Kaul R, Virji M, Gray-Owen SD. Selection for a CEACAM receptor-specific binding phenotype during *Neisseria gonorrhoeae* infection of the human genital tract. Infect Immun 2015;83(4):1372–1383. [PubMed: 25605771]
33. Popp A, Dehio C, Grunert F, Meyer TF, Gray-Owen SD. Molecular analysis of neisserial Opa protein interactions with the CEA family of receptors: Identification of determinants contributing to the differential specificities of binding. Cell Microbiol 1999;1(2):169–181. [PubMed: 11207550]
34. Delgado Tascon J, Adrian J, Kopp K, Scholz P, Tschan MP, Kuespert K, Hauck CR. The granulocyte orphan receptor CEACAM4 is able to trigger phagocytosis of bacteria. J Leukoc Biol 2015;97(3):521–531. [PubMed: 25567962]
35. Gorgens A, Bremer M, Ferrer-Tur R, Murke F, Tertel T, Horn PA, Thalmann S, Welsh JA, Probst C, Guerin C, et al. Optimisation of imaging flow cytometry for the analysis of single extracellular vesicles by using fluorescence-tagged vesicles as biological reference material. J Extracell Vesicles 2019;8(1):1587567. [PubMed: 30949308]
36. Fox DA, Larsson P, Lo RH, Kroncke BM, Kasson PM, Columbus L. Structure of the Neisserial outer membrane protein Opa(6)(0): Loop flexibility essential to receptor recognition and bacterial engulfment. J Am Chem Soc 2014;136(28): 9938–9946. [PubMed: 24813921]
37. Dehio M, Gómez-Duarte OG, Dehio C, Meyer TF. Vitronectin-dependent invasion of epithelial cells by *Neisseria gonorrhoeae* involves alpha(v) integrin receptors. FEBS Lett 1998;424(1–2):84–88. [PubMed: 9537520]
38. Stevens JS, Gray MC, Morisseau C, Criss AK. Endocervical and neutrophil lipoxygenases coordinate neutrophil transepithelial migration to *Neisseria gonorrhoeae*. J Infect Dis 2018;218(10):1663–1674. [PubMed: 29905822]
39. Boulton IC, Gray-Owen SD. Neisserial binding to CEACAM1 arrests the activation and proliferation of CD4+ T lymphocytes. Nat Immunol 2002;3(3):229–236. [PubMed: 11850628]

40. Kammerer R, Zimmermann W. Coevolution of activating and inhibitory receptors within mammalian carcinoembryonic antigen families. BMC Biol 2010;8:12. [PubMed: 20132533]

41. Adrian J, Bonsignore P, Hammer S, Frickey T, Hauck CR. Adaptation to host-specific bacterial pathogens drives rapid evolution of a human innate immune receptor. Curr Biol 2019;29(4):616–630 e5. [PubMed: 30744974]

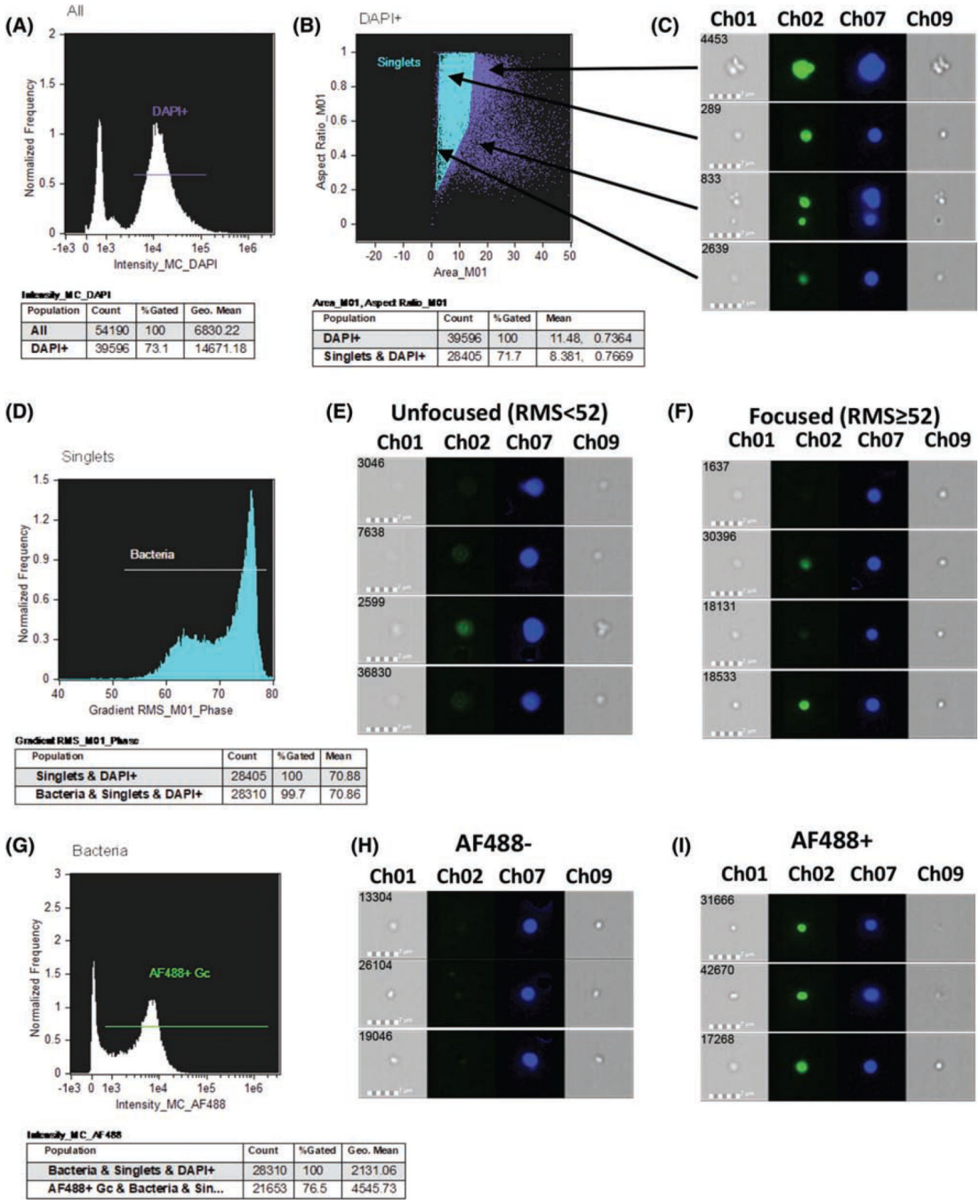

Population	Count	%Gated	Geo. Mean
All	54190	100	6830.22
DAPI+	39596	73.1	14671.18

Population	Count	%Gated	Mean
DAPI+	39596	100	11.48, 0.7364
Singlets & DAPI+	28405	71.7	8.381, 0.7669

Population	Count	%Gated	Mean
Singlets & DAPI+	28405	100	70.88
Bacteria & Singlets & DAPI+	28310	99.7	70.86

Population	Count	%Gated	Geo. Mean
Bacteria & Singlets & DAPI+	28310	100	2131.06
AF488+ Gc & Bacteria & Sin...	21653	76.5	4545.73

Fig 1.

Gating strategy. Gc was incubated with purified recombinant GST-N-CEACAM3 (CCM3), washed, and stained with anti-GST antibody, followed by anti-mouse-AF488 secondary antibody. Stained bacteria were fixed in PBS containing 2% PFA and 5 μg/ml DAPI. (**A**) Bacteria were defined as particles with high DAPI intensity. (**B**) Single bacteria were identified from DAPI+ population. (**C**) Examples of single and clumped bacteria. (**D**) Focused bacteria were defined as particles with RMS ≥52. (**E**) and (**F**) Examples of bacteria

out of focus (E) and focused (F). (**G**) AF488+ Gc gate includes bacteria with high AF488 fluorescence intensity. (**H**) and (**I**) examples of AF488-negative (H) and positive (I) bacteria.

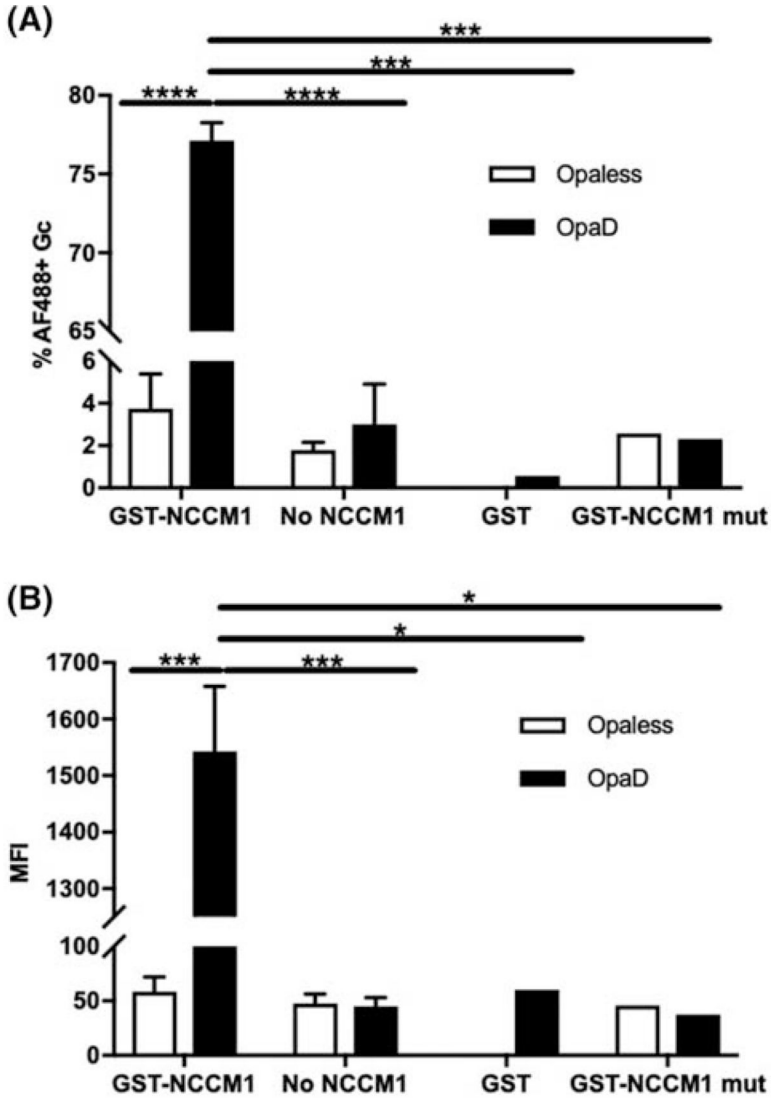

Fig 2.

Imaging flow cytometry can detect the binding of N-CEACAM-1 to Opa-expressing Gc. OpaD+ or Opaless Gc was incubated with GST-tagged N-CEACAM1 (GST-NCCM1), an N-CEACAM-1 mutant where the binding interface for Opa proteins was disrupted (GST-NCCM1 Mut; point mutations I87A/Q89A/I91A), GST alone, or no protein (no NCCM1). After washing, bacteria were fixed and stained with mouse anti-GST followed by AF488-coupled anti-mouse, along with DAPI. The (**a**) percentage of DAPI+ Gc that are AF488-positive and (**b**) MFI of AF488 for DAPI+ Gc was quantified using imaging flow cytometry using the gating strategy in Figure 1. Results presented are the mean ± standard error of the mean. $N \geq 3$ (except for GST alone, $n = 1$). ***$P < 0.001$, ****$P < 0.0001$ (Student's two-tailed unpaired t test).

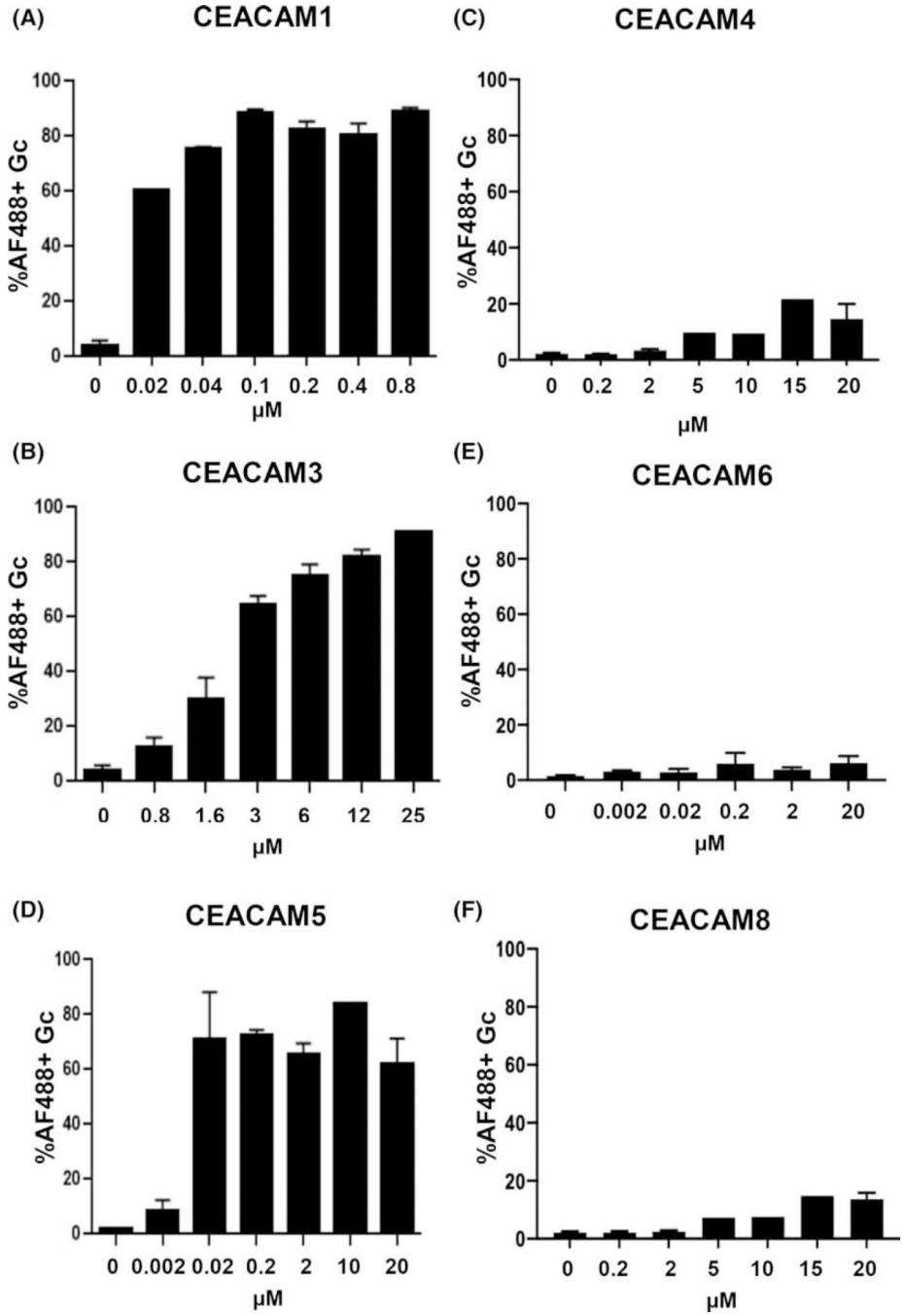

Fig 3.

Determination of the optimal final working concentration for N-CEACAMs. OpaD+ Gc was incubated with increasing concentrations of each of the recombinant GST-N-CEACAM proteins indicated. Depicted are final concentrations for each protein. Bacteria were processed for imaging flow cytometry as described in Figures 1 and 2. Results are presented as percent of AF488+ bacteria (similar results were obtained for MFI). Results presented are the mean ± standard error of the mean. N = 1–6 experiments.

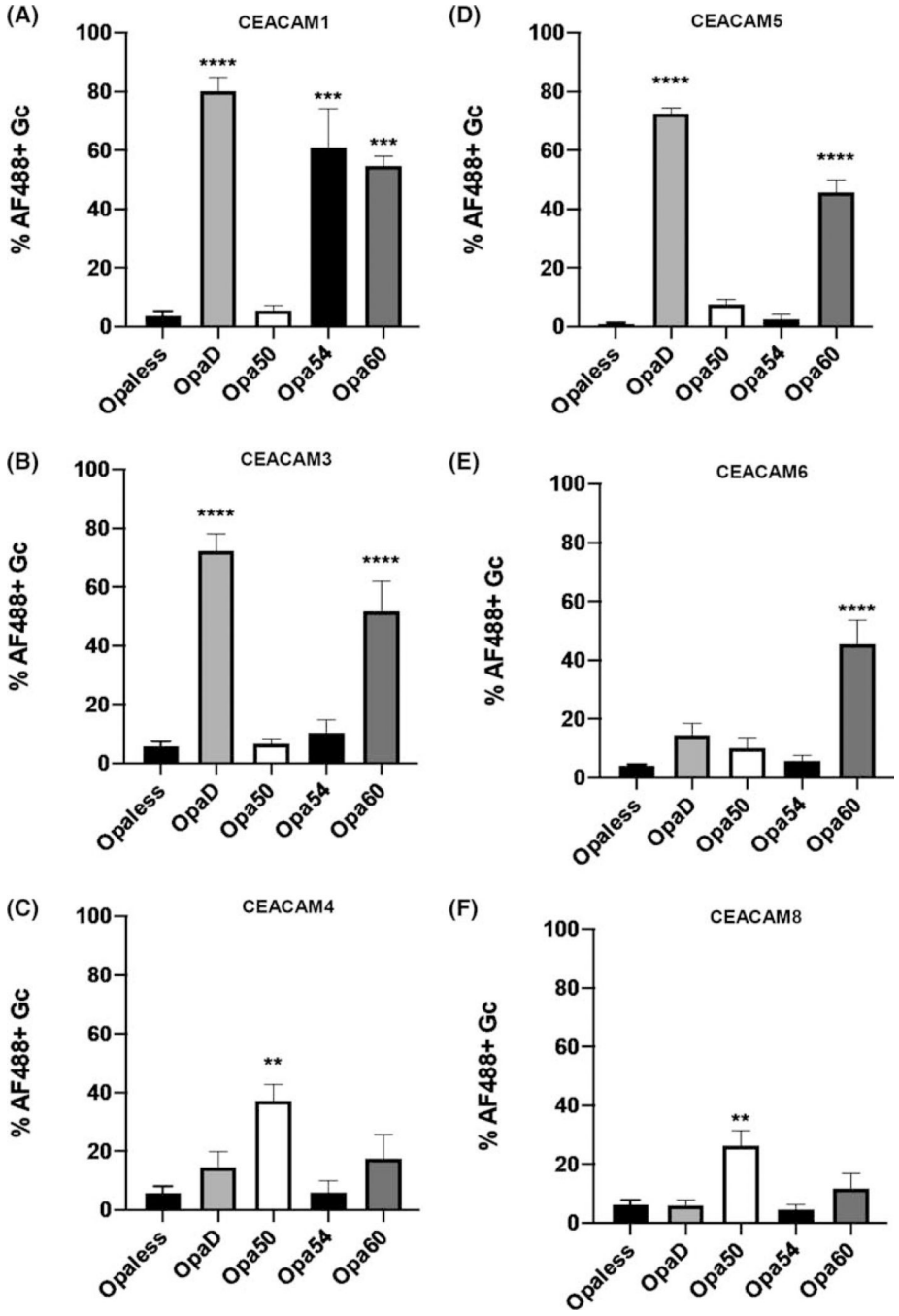

Fig 4.

CEACAM binding profiles of Opa proteins. The binding of Opa + Gc to each of six recombinant N-CEACAMs was determined by imaging flow cytometry as in Figures 1 and 2, using the concentration of each GST-N-CEACAM determined for OpaD+ Gc in Figure 3. Opaless served as a negative control for background AF488+ fluorescence on bacteria and was used as comparison for statistical significance. Results are presented as percent of AF488+ bacteria (similar results were obtained for MFI). Results presented are the mean ±

standard error of the mean. $N = 3–6$ experiments. $^{**}P < 0.01$, $^{***}P < 0.001$, $^{****}P < 0.0001$ (one-way ANOVA with post hoc multiple comparisons).